Effect of Cholesterol on the Phase Behavior of Solid-Supported Lipid Vesicle Layers

ARTICLE *in* THE JOURNAL OF PHYSICAL CHEMISTRY B · MARCH 2015

Impact Factor: 3.3

4 AUTHORS, INCLUDING:

Patricia Losada-Pérez

Hasselt University

40 PUBLICATIONS **303** CITATIONS

SEE PROFILE

Mehran Khorshid

University of Leuven

6 PUBLICATIONS **6** CITATIONS

SEE PROFILE

Patrick Wagner

University of Leuven

264 PUBLICATIONS **2,650** CITATIONS

SEE PROFILE

THE JOURNAL OF PHYSICAL CHEMISTRY B

Article

pubs.acs.org/JPCB

Effect of Cholesterol on the Phase Behavior of Solid-Supported Lipid Vesicle Layers

P. Losada-Pérez,*[,†,‡] M. Khorshid,[†,§] D. Yongabi,[†] and P. Wagner[†,§]

[†]Institute for Materials Research IMO, Hasselt University, Wetenschapspark 1, B-3590, Diepenbeek, Belgium

[‡]Division IMOMEC, IMEC vzw, Wetenschapspark 1, B-3590, Diepenbeek, Belgium

[§]Soft Matter and Biophysics Section, Department of Physics and Astronomy, KU Leuven, Celestijnenlaan 200D bus 2416, B-3001, Leuven, Belgium

Supporting Information

ABSTRACT: The interest in solid-supported biomimetic membranes stems from their utility in nanotechnology and biosensing. In particular, supported lipid vesicles (SLVs) have become popular in both fundamental biophysical studies and pharmaceutical screening applications. It is thus essential to gain information on the structural properties and phase behavior of SLVs. Here we report on a study on the influence of cholesterol on the phase behavior of SLVs of saturated phospholipids by using quartz crystal microbalance with dissipation monitoring, a label-free and nonintrusive surface-sensitive technique. Two complementary approaches have been used, a Voigt-based viscoelastic model yielding shear viscosity temperature profiles and the first-order derivative of the frequency (mass-sensitive) shifts. Anomalies in the shear viscosity and extrema in the first-order derivative frequency curves stand as a token of the main phase transition and provide information on its gradual suppression upon addition of cholesterol. This method proves convenient for its small sample volume needed, its short temperature equilibration time and the non-necessity of external labels. This work can be regarded as a starting point for further studies on more rare lipid systems and different geometries, such as tethered SLVs or biologically relevant vesicles produced by living cells.

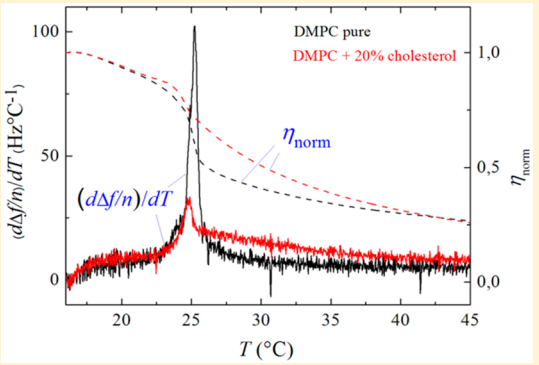

INTRODUCTION

Cholesterol is a lipid from the family of sterols whose presence is ubiquitous in eukaryotic cell plasma membranes. Its molecular characteristics give cholesterol unique properties that motivated intensive research in the last decades, especially on its role in structure and function of lipid bilayer membranes, both natural and model ones.[1−7] Cholesterol has the ability to control the lateral organization of membranes, providing mechanical strength and imparting low permeability barriers to lipid membranes by controlling fluidity and thickness.[8−11] The presence of cholesterol is intimately related to the lipid raft hypothesis.[12−14] Lipid rafts correspond to membrane areas stabilized by cholesterol within a more ordered phase and may serve as platforms for cell signaling and membrane trafficking. As a matter of fact, their existence has motivated a plethora of studies to investigate the influence of lipid rafts on interactions of model membranes with biomolecules such as peptides and nucleic acids (see, for instance, refs 15−20).

In this regard, the study of the behavior of static and dynamic thermodynamic properties of model membranes is fundamental for a better understanding of the phase behavior of cholesterol-containing lipid systems. The influence of cholesterol on lipid phases has been studied for free-standing lipid bilayers systems using several experimental techniques such as calorimetry,[21−24] nuclear magnetic resonance (NMR),[25−30] electron spin resonance,[31] X-ray diffraction,[32,33] fluorescence microscopy,[34] laser ultrasonics,[35] and partial volume measurements[36] as well as by molecular simulations.[37−39] Although the effect of cholesterol depends on the type of lipid, a standard dual behavior of cholesterol is observed above and below the melting temperature T_m of the lipid bilayer: it promotes ordering of the alkyl chains above T_m and disorder below T_m. As a result, cholesterol induces the appearance of the liquid-ordered phase, which shares features of both the gel and the liquid-disordered phases.[40−42]

Despite the vast number of studies on the phase behavior of free-standing lipid systems, the interest in the phase behavior of different lipid geometries such as solid-supported lipid layers is emerging and motivated by their utility in nanotechnology and biosensing.[43] The most commonly used solid-supported systems are supported lipid bilayers (SLBs), supported layers of vesicles (SLVs) and supported lipid monolayers. The influence of cholesterol on solid-supported lipid layers has been examined for supported lipid bilayers (SLBs) and lipid

Received: January 23, 2015
Revised: March 25, 2015
Published: March 26, 2015

DOI: 10.1021/acs.jpcb.5b00712
J. Phys. Chem. B 2015, 119, 4985−4992

monolayers (SLMs) by atomic force microscopy AFM-based force spectroscopy and microcantilevers, respectively.[44,45] In turn, to the best of our knowledge, there is no phase transition study on SLVs containing cholesterol until date.

In view of the lack of experimental studies on SLVs, we have used quartz crystal microbalance with dissipation monitoring (QCM-D) to examine the phase behavior of cholesterol-containing SLVs and the influence of substrate interactions. QCM-D has been mainly used to characterize vesicle adsorption kinetics and formation of SLBs and bilayer-protein interactions, see, for instance refs 46−48. Only recently, it was proposed as a method to study structural layer changes upon the main phase transition of phospholipid layers.[49−54] We have chosen two phospholipids differing in two ethyl groups, namely, dipamitoylphosphatidylcholine (DPPC) and dimirystoilphosphatidylcholine (DMPC). Using QCM-D, we present two different ways of analyzing phase transitions of cholesterol containing SLVs. On the one hand, we apply a Voigt-based viscoelastic model to obtain the shear viscosity temperature profile and analyze its changes upon the main phase transition. On the other hand, we calculate the temperature derivative of the directly measured frequency shift response. Results indicate that the two approaches yield consistent and complementary information on the cholesterol-induced changes on the phase transition and viscoelastic properties of the lipid layers under study. Unlike SLBs, the presence of a solid support hardly affects the phase behavior of SLVs as compared to free-standing lipid bilayers.

EXPERIMENTAL METHODS

Materials. DMPC, DPPC, and cholesterol were purchased from Avanti Polar Lipids (Alabaster, AL). Spectroscopic grade chloroform (assay 99.3% stabilized with about 0.6% ethanol) was obtained from Analar (Normapur). HEPES buffer (pH 7.4) consisting of 10 mM HEPES from Fisher Scientific (assay 99%) and 150 mM NaCl from Sigma-Aldrich (assay ≥99.5%) was used for hydration of the dried lipids. The quantities of lipids to reach the desired mixture concentrations were determined gravimetrically using a Sartorius balance yielding a maximal mole fraction uncertainty of ±0.002.

Vesicle Preparation. The lipid or lipid mixture was first dissolved in spectroscopic grade chloroform and the solvent was then evaporated under a mild flow of nitrogen in a round bottomed flask. The resulting lipid film was kept under vacuum overnight to remove residual solvent. Then, the lipid was hydrated with HEPES buffer. Hydration to 1 mg/mL was carried out under continuous stirring in a temperature-controlled water bath at sufficiently high temperature (45 °C for DMPC-containing systems and 60 °C for DPPC-containing systems, both around 20 °C above their respective main phase transition temperatures T_m). Small unilamellar vesicles (SUVs) were formed by extrusion through a filter support (Avanti Polar Lipids) with a pore size of 100 nm for 25 times. Vesicle effective sizes and polydispersities were determined by dynamic light scattering (Zeta Pals, Brookhaven Instruments Corporation). The obtained average diameter was ∼130 ± 30 nm. The obtained average diameters and polydispersities of the samples used are displayed in Table 1. The vesicle dispersions were stored at 4 °C and used within 2 days.

Quartz Crystal Microbalance with Dissipation. Quartz crystal microbalance with dissipation monitoring (QCM-D) is an acoustic surface-sensitive technique based on the inverse piezoelectric effect. The application of an ac voltage over the sensor electrodes causes the piezoelectric quartz crystal to oscillate at its acoustic resonance frequency. As a result, a transverse acoustic wave propagates across the crystal, reflecting back into the crystal at the surface. When the ac voltage is turned off, the oscillation amplitude decays exponentially, this decay is recorded and the frequency (f) and the energy dissipation factor (D) of different overtones are extracted.[46] The dissipation D is the ratio between the dissipated energy during one vibration cycle and the total kinetic and potential energy of the crystal at that moment.

Table 1. Average Diameters and Polydispersities of the Samples under Study[a]

sample	d (nm)	polydispersity
DMPC	124	0.04
DMPC + 5% cholesterol	126	0.06
DMPC + 10% cholesterol	127	0.06
DMPC + 15% cholesterol	130	0.10
DMPC + 20% cholesterol	131	0.09
DMPC + 30% cholesterol	162	0.18
DPPC	130	0.08
DPPC + 5% cholesterol	136	0.10
DPPC + 10% cholesterol	143	0.10
DPPC + 15% cholesterol	140	0.12
DPPC + 20% cholesterol	152	0.12
DPPC + 30% cholesterol	169	0.23

[a]Percentages are given in mass.

When molecules adsorb to an oscillating quartz crystal, water (or buffer) couples to the adsorbed material as an additional dynamic mass via direct hydration and/or entrapment within the adsorbed film. The layer is thus sensed as a viscoelastic hydrogel composed of the molecules and the coupled water together. In our case, it was especially useful to monitor the formation of an intact vesicle layer, since it senses the water coupled to the adsorbed layer. The adsorbed layer is described by a frequency-dependent complex shear modulus, defined as[55,56]

$$G = G' + iG'' = \mu_l + 2\pi i f \eta_l = \mu_l(1 + 2\pi i \chi) \quad (1)$$

where G' and G'' stand for energy storage and dissipation, respectively, f is the oscillation frequency, μ_f is the elastic shear storage modulus, η_l is the shear viscosity, and $\chi = \mu_f/\eta_f$, is the relaxation time of the layer.

For the current measurements, we have used QCM-D on a Q-sense E4 instrument (Gothenborg, Sweden) monitoring the frequency shift Δf and the dissipation change ΔD. Q-sense E4 also enables heating or cooling temperature scans from 15 to 50 °C. AT-cut quartz crystals with Au coating (diameter 14 mm, thickness 0.3 mm, surface roughness 3 nm and resonant frequency 4.95 MHz) were used. The Au-coated quartz sensors were cleaned with a 5:1:1 mixture of Milli-Q water (conductivity of 0.055 S cm^{-1} at 25 °C), ammonia and hydrogen peroxide, and were UV-ozone treated with a Digital PSD series UV-ozone system from Novascan for 15 min, followed by rinsing in milli-Q water and drying with N_2. The changes in $\Delta f/n$ and in ΔD were monitored at five different overtones (from third to 11th, the fundamental frequency is rather unstable since this is the one that reaches the farthest out to the edge of the sensor and may be therefore affected by the O-ring). First, a baseline with pure HEPES buffer was established and afterward lipid vesicles were injected over the sensor chip with a flow rate of 50 μL/min. After 15 min the

DOI: 10.1021/acs.jpcb.5b00712
J. Phys. Chem. B 2015, 119, 4985−4992

pump was switched off. Subsequent temperature scans with alternating heating and cooling were performed at a rate of 0.2 °C/min, maintaining 60 min of stabilization between successive ramps. The temperature stability at constant temperature was ±0.02 °C.

RESULTS AND DISCUSSION

Lipid Layer Formation. The lipid layer formation depends on the vesicle−vesicle interactions and vesicles-substrate interactions that influence the deformation behavior of the vesicles adsorbed. The factors that rule the type of lipid layer formed (SLB or SLV) are substrate properties, temperature of deposition and composition of the layer.[46,57−59] As a consequence, vesicle dispersions were adsorbed onto gold substrates at temperatures well below the main transition temperature of the pure phospholipid. DMPC−cholesterol and DPPC−cholesterol systems were deposited at 16 and 25 °C, respectively. The curvature bending modulus at low temperature (gel phase) is higher than that above the melting temperature (liquid disordered phase), promoting the formation of a stable vesicle layer. Vesicle deposition takes places reaching a stable plateau at large Δf and ΔD values in all the studied systems. The fact that the different overtones do not overlap denotes the deposition of an acoustically nonrigid vesicle layer both for DMPC and DPPC containing systems (see Figure 1 in the Supporting Information). The $\Delta D-\Delta f$ plots in Figure 1 show the influence of cholesterol on vesicle adsorption. In general, on increasing the amount of cholesterol, a higher surface coverage of vesicles is required (larger Δf and thus larger mass) and the layers display a larger energy dissipation. Due to its small polar head, cholesterol can flip-flop faster between the two bilayer leaflets, helping to accommodate vesicle deformation and stabilizing flattened vesicles on the surface. This applies to both DMPC and DPPC cholesterol mixtures.

After a stable vesicle layer is formed, heating and cooling runs were performed at a rate of 0.2 °C/min. Reference tests were performed simultaneous thanks to four QCM-D modules. Figure 2 shows a comparison of the frequency and dissipation shift responses of the sensors only exposed to HEPES buffer (reference sensor) and the sensor containing an adsorbed pure DMPC vesicle layer as example, DPPC exhibits an analogous behavior. The former exhibits the expected regular behavior; i.e., frequency/dissipation shift increases/decreases with in-

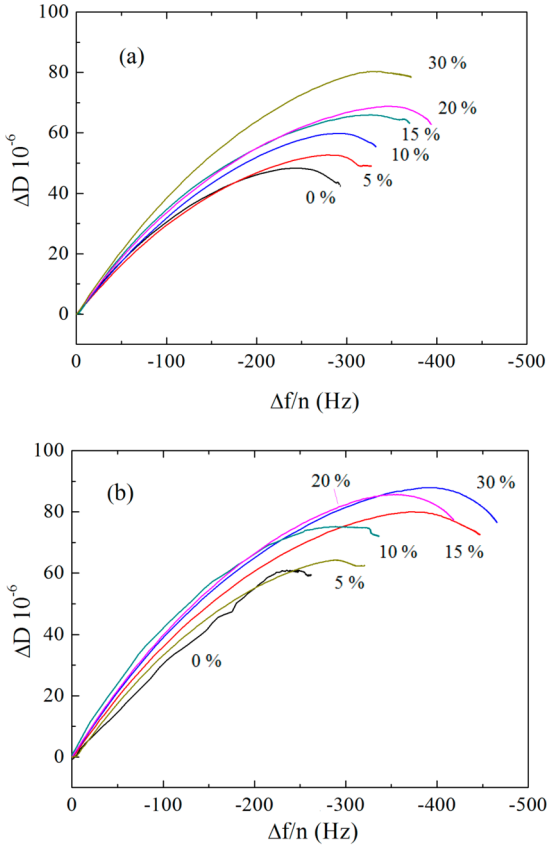

Figure 1. $\Delta D-\Delta f/n$ plots for the 9th overtone. (a) DMPC + cholesterol and (b) DPPC + cholesterol systems.

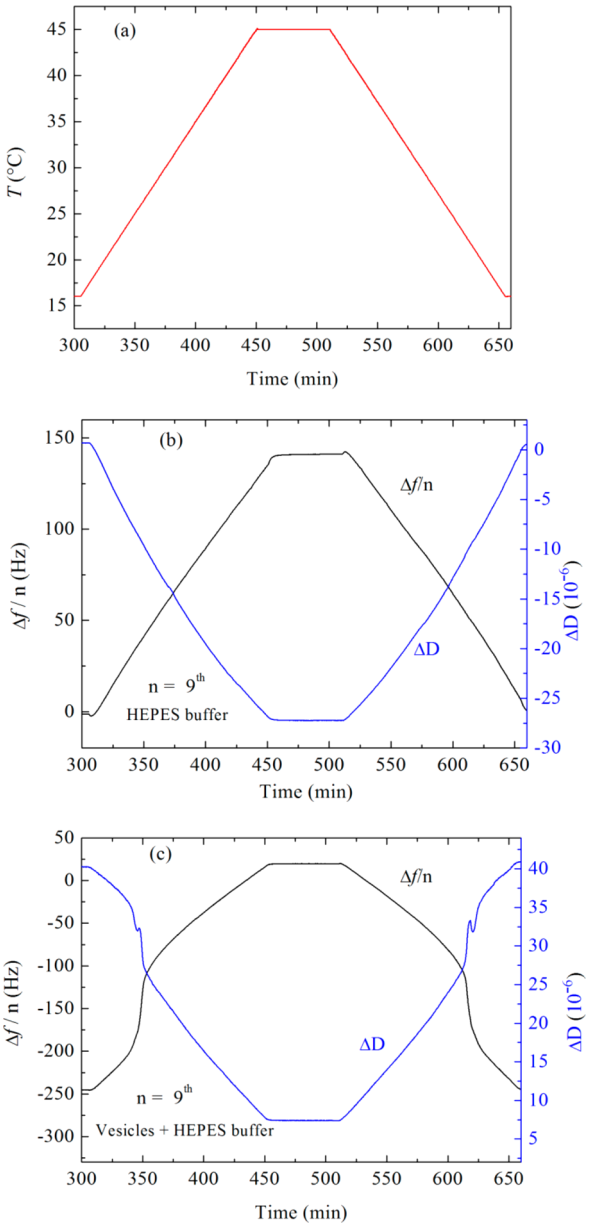

Figure 2. Upper panel (a): Temperature vs time. Middle and low panel: 9th overtone $\Delta f/n$ (black solid line) and ΔD (blue solid line) vs time for (b) a blank QCM-D sensor with HEPES buffer and (c) sensor with HEPES buffer and vesicles adsorbed. Results correspond to a pure DMPC vesicle layer.

DOI: 10.1021/acs.jpcb.5b00712
J. Phys. Chem. B 2015, 119, 4985−4992

creasing temperature, while the latter displays anomalies in both frequency and dissipation responses. Specifically, close to the main phase transition temperature, both frequency and the dissipation responses deviate from the regular behavior upon temperature change far for the transition. Such anomalies reveal that structural changes are taking place and constitute a fingerprint of thermotropic phase transitions.

Viscoelastic Analysis. We have used a Kelvin−Voigt based model introduced by Voinova et al. assuming that the vesicle layer has uniform thickness, film density, Newtonian bulk fluid and no-slip conditions (perfect coupling onto the quartz sensor). As a result, $|\Delta f/n|$ and ΔD can be expressed in terms of the film density ρ_f, viscosity η_f and thickness h_f:[55,56]

$$\Delta f \cong \frac{1}{2\pi\rho_q h_q} h_f \rho_f \omega \left(1 + \frac{2h^2\chi}{3\delta^2(1+\chi^2)}\right) \quad (2)$$

$$\Delta D \cong \frac{2t^3\rho_f f}{3\pi f_0 \rho_q h_q}\left(\frac{1}{\delta^2(1+\chi^2)}\right) \quad (3)$$

$$\tan\delta = \frac{1}{\chi}\left(\frac{2\pi f\eta_l}{\mu_l}\right) \quad (4)$$

$$\delta = \sqrt{\frac{2\eta_l}{\rho_l f}} \quad (5)$$

where f is the frequency of a given overtone, f_0 is the fundamental frequency, $\omega = 2\pi f$, h denotes thickness of the quartz and μ shear modulus and δ is referred to the penetration depth of a propagating shear wave into the vesicle film. The subscripts q and f refers to quartz and to the vesicle layer, respectively. χ the ratio between μ_f and η_f. The data of several overtones (3rd to 11th) were fitted using the software Qtools (Q-Sense AB, Sweden) keeping as fixed parameters the density of the lipid layer 1.06 g·cm^{-3},[59] the density of the fluid 1.0 g·cm^{-3} and the viscosity of the fluid 1 mPa·s. The viscosity values should be taken as effective and not as absolute values because the model assumes a homogeneous vesicle layer and our vesicle dispersions were not perfectly monodisperse. Figure 3 displays the temperature dependence of the shear viscosity of pure DMPC upon heating and cooling. Upon cooling, the viscosity responses show a similar shape as upon heating with ∼1.5 K hysteresis, a characteristic feature of first-order transitions.[60] The observed hysteresis is temperature dependent and might by partly ascribed to gradients inside the flow cell. As it can be observed, the change from the gel state to the liquid-disordered state is reflected in the viscosity behavior, which decreases from a more viscous state (gel phase) to a less viscous one (liquid-disordered). At a given temperature, where the phase transition starts, a sudden decrease in η is observed. Once all the lipid molecules have completed the phase conversion, a regular behavior is recovered since all lipids are in the liquid-disordered phase. The temperatures at which the transition takes place are slightly higher than the ones observed by DSC.[22−25] This might be due to presence of the solid substrate, as observed for supported lipid bilayers;[61] however, the fact that the viscosity change is at slightly higher temperature than the phase transition, or that the model does not apply because of the presence of ripples cannot be ruled out. Figure 4 displays the

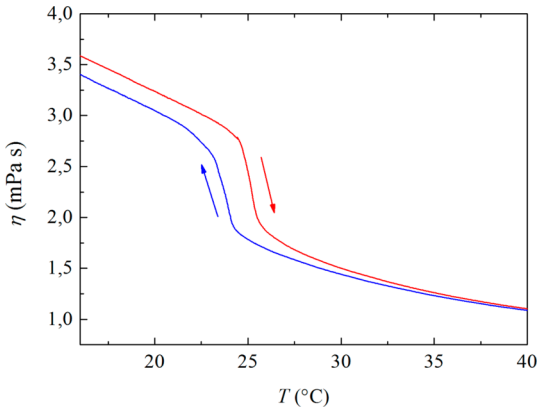

Figure 3. Temperature dependence of the calculated shear viscosity of a DMPC SLV layer on a gold-coated quartz crystal. The red solid line represents "upon heating", while the blue solid line represents "upon cooling".

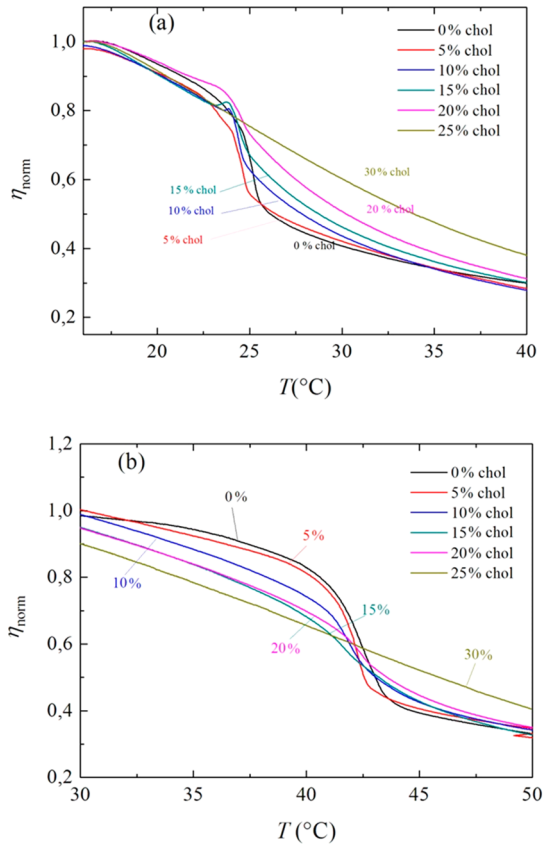

Figure 4. Temperature dependence of the calculated effective viscosity η_{norm} normalized as $\eta_{norm} = (\eta(t))/(\eta(t=0))$ of a supported vesicle layer on a gold-coated QCM-D quartz sensor. (a) DMPC + cholesterol mixtures; (b) DPPC + cholesterol mixtures.

temperature dependence of the normalized effective viscosity $\eta_{norm} = (\eta(t))/(\eta(t=0))$ for all the studied compositions upon heating. For mixtures containing cholesterol, the transition takes place in a wider temperature range and the jump in $\eta(T)$ changes from a steeper to a shallower slope during the transition indicating the presence of two contributions. The steep slope accounts for the transition of pure lipid-rich domains, whereas the shallow slope corresponds to cholesterol-rich domains. Upon increasing cholesterol concentration, the temperature range of the shallow slope increases, indicating the

DOI: 10.1021/acs.jpcb.5b00712
J. Phys. Chem. B 2015, 119, 4985−4992

loss of the intermolecular cooperation between phospholipid molecules in the bilayer or *cooperativity*. At 30% cholesterol, there is no jump in $\eta(T)$ and so no transition is detectable, in agreement to what it is observed from calorimetric measurements in ref 24. Although the values of viscosity are not absolute, the trend observed on increasing cholesterol agrees with the dual effect of cholesterol above and below the T_m of the pure phospholipid. In our results, the effect is more substantial above T_m, where cholesterol promotes ordering of the alkyl chains and thus viscosity increases, while below T_m it tends to "fluidize" the bilayer. At this point, it is worth mentioning that despite the fact that we would expect a lower temperature transition from a gel to a ripple phase in both types of pure phospholipids and mixtures, there is no indication of it from the viscosity−temperature curve.

Frequency Derivative Analysis. As mentioned above, the signature of the phase transition is characterized by an anomalous behavior in the frequency and dissipation shift responses. An alternative way of looking at the phase transition is thus to plot the temperature derivative of the frequency and dissipation curves. Figure 5 shows an example of Δf and its

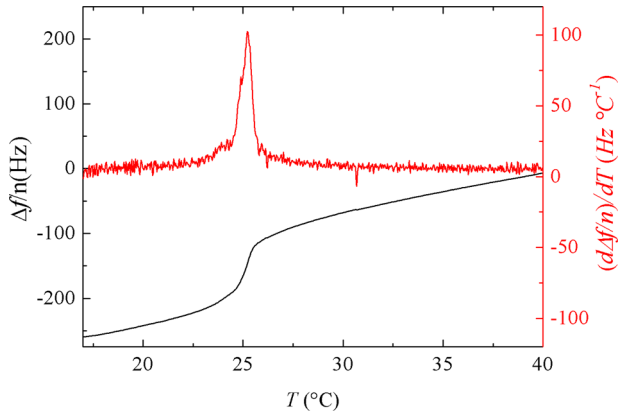

Figure 5. Temperature dependence of the frequency shift (black solid line) and its first-order derivative (red solid line) of a DMPC layer upon heating.

temperature derivative $d\Delta f/dT$ for pure DMPC upon heating, where the jump in $\Delta f(\Delta D)$ corresponds to a maximum (minimum) in $(d\Delta f/n)/dT$ ($d\Delta D/dT$) curve. The advantage of plotting the derivative is that, unlike $\eta(T)$ curves, the determination of the onset and completion temperatures is more straightforward. In addition, the size of the maximum is several orders of magnitude larger than the one observed in SLBs.[53] Interestingly enough, the shape of the frequency shift curves is reminiscent of the enthalpy jump and its heat capacity derivative from calorimetric measurements.[22−25] In fact, the half-width of the maximum is of the order of the one obtained by calorimetric measurements (~ 0.65 °C), indicating that the transition in pure DMPC is highly cooperative.[54] The effect of cholesterol on the main phase transition of both DMPC and DPPC is depicted in Figure 6. Two main effects are observed: upon addition of cholesterol T_m is shifted to slightly lower values and levels off and slightly increases from 15% cholesterol (especially for DPPC mixtures) at high cholesterol concentrations. This phase transition temperature shifts differ with some calorimetric measurements,[23,24] while they agree with previous fluidity experiments.[62] A review of this differing behavior is included in ref 63. Moreover, the height of the peak

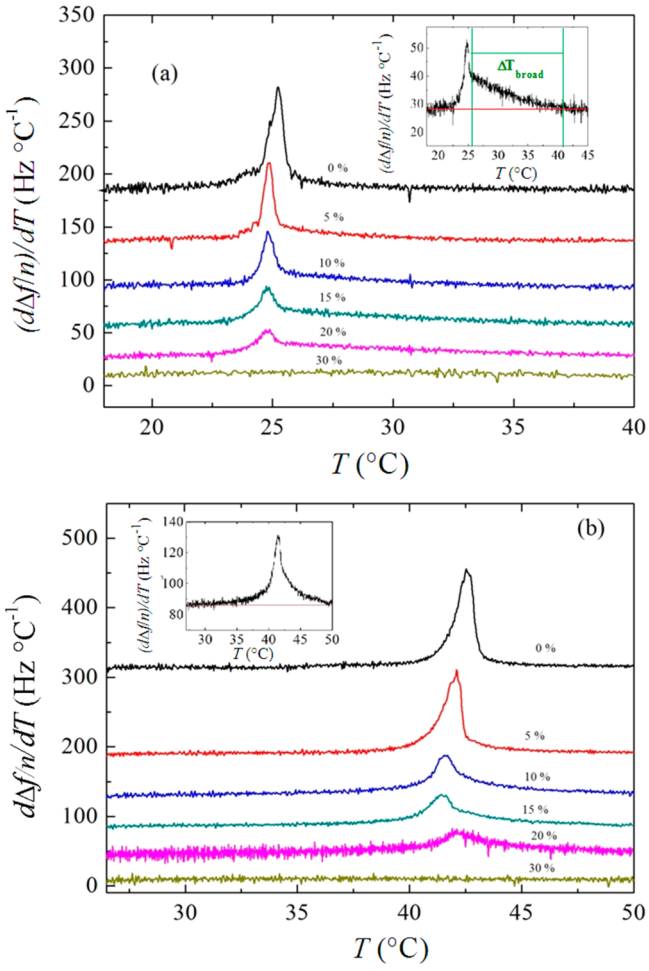

Figure 6. Temperature profiles of the first-order temperature derivative of the frequency shifts. (a) DMPC + cholesterol systems, the inset represents the mixture with 20% cholesterol and (b) DPPC + cholesterol systems, the inset represents the mixture with 15% cholesterol. For clarity the curves have vertically shifted a constant amount and the insets have the same units as the main plots. For DMPC + chol inset, the broad peak temperature range is delimited with green lines.

decreases and its temperature width increases, indicating that the phase transition is gradually suppressed. As a matter of fact, the maximum encompasses two main contributions, a sharp, narrow peak and a broader one (see insets of Figure 6 for a more detailed view). The former can be ascribed to the pure lipid-rich domains and the latter to the cholesterol-rich ones, in analogy with the different slopes observed in $\eta(T)$ curves. The horizontal lines in Figure 6 are used as guide to the eye to delimit the onset and completion temperatures and to evaluate the range of extension of the second broader contribution of cholesterol rich domains. On increasing the amount of cholesterol, the temperature range of the overall transition increases as a result of the extension of the second broad contribution, while the size of the maximum corresponding to the melting of the single lipid decreases (Figure 2 of the Supporting Information). These results are in agreement with calorimetric studies of free-standing membranes of the same systems.[22−25]

DOI: 10.1021/acs.jpcb.5b00712
J. Phys. Chem. B 2015, 119, 4985−4992

CONCLUSIONS

The influence of cholesterol on the phase behavior of solid-supported vesicle layers of phosphatidylcholines has been evaluated using two complementary approaches: Voigt-based viscoelastic modeling and the temperature derivative of the frequency (mass sensitive) shifts. The former yields shear viscosity temperature profiles that display a clear signature of the main phase transition and its evolution upon cholesterol addition. Besides, the dual effect of cholesterol on membrane fluidity above and below the main phase transition temperature of the pure lipids is clearly observed. In the latter approach the phase transition is reflected by extrema in $d\Delta f/dT$ upon heating and cooling, making the determination of the onset and completion temperatures more straightforward and subjected to a smaller uncertainty. In both approaches, two contributions can be detected in cholesterol-containing systems, corresponding to the coexistence of pure phospholipid-rich and cholesterol-rich domains. Upon the addition of cholesterol, the gradual increase of the latter and loss of cooperativity is observed, indicating the formation of a single homogeneous liquid-ordered phase. The results obtained indicate that the presence of the solid substrate might induce slightly higher main transition temperatures of supported lipid vesicles of ~100 nm as compared to free-standing ones.

In summary, we have validated QCM-D as an alternative but simple way to study the phase behavior of cholesterol-containing biomimetic membranes. QCM-D is advantageous for its small sample quantity needed, low temperature equilibration time and no need for labeling molecules. This method is applicable for phospholipids exhibiting low melting temperatures like DOPC, provided that an external cooling stage and corresponding temperature control is incorporated in the setup to more complex systems like antimicrobial or amyloid peptide's influence on the lipid phase behavior, peculiar lipids and lipid geometries, i.e., tethered lipid vesicle layers or supported lipid bilayers.

ASSOCIATED CONTENT

Supporting Information

(1) Frequency and dissipation responses upon the formation of a layer of lipid vesicles and (2) the cholesterol dependence of the temperature ranges of the observed transitions. This material is available free of charge via the Internet at http://pubs.acs.org.

AUTHOR INFORMATION

Corresponding Author

*(P.L.-P.) Telephone: 0032 11268876. E-mail: patricia.losadaperez@uhasselt.be.

Notes

The authors declare no competing financial interest.

ACKNOWLEDGMENTS

This work was supported by The Belgian Province of Limburg in the framework of "Life-Science Initiative", the Flemish Government in the framework of the Methusalem project NANO Hasselt-Antwerp, The Research Foundation Flanders FWO, project 6.0B62.13N and Special Research Funds BOF of Hasselt University. The authors thank Prof. Marlies Van Bael for authorizing the use of DLS. P.L.-P. acknowledges George Cordoyiannis for stimulating scientific discussions. We thank the reviewers for constructive remarks and suggestions.

REFERENCES

(1) Oldfield, E.; Chapman, D. Dynamics of lipids in membranes: Heterogeneity and the role of cholesterol. *FEBS Lett.* **1972**, *23*, 285–297.
(2) Trentacosti-Presti, F. *Membrane fluidity in Biology*, Aloia, R. C., Boggs, J. M., Ed.; Academic Press: London, 1985; Vol. *4*, Chapter 3.
(3) Mouritsen, O. G.; Zuckermann, M. J. What's so special about cholesterol? *Lipids* **2004**, *39*, 1101–1113.
(4) Mouritsen, O. G. *Life–As a matter of fat: The emerging science of lipidomics*; Springer-Verlag: Heidelberg, Germany, 2005.
(5) Mouritsen, O. G. Lipidology and lipidomics–Quo vadis? A new era for the physical chemistry of lipids. *Phys. Chem. Chem. Phys.* **2011**, *13*, 19195–19205.
(6) Epand, R. F.; Ramamoorthy, A.; Hancock, R. E. W. Membrane lipid composition and the interaction of pardaxin: The role of cholesterol. *Protein Pept. Lett.* **2006**, *13*, 1–5.
(7) Henzler-Wildman, K. A.; Martínez, G. V.; Brown, M. F.; Ramamoorthy, A. Perturbation of the hydrophobic core of lipid bilayers by the human antimicrobial peptide LL-37. *Biochemistry* **2004**, *43*, 8459–8469.
(8) Hung, W. C.; Lee, M. T.; Chen, F. Y.; Huang, H. W. The condensing effect of cholesterol in lipid bilayers. *Biophys. J.* **2007**, *92*, 3960–3967.
(9) Pan, J.; Tristam-Nagle, S.; Nagle, J. F. Effect of cholesterol on structural and mechanical properties of membranes depends on lipid chain saturation. *Phys. Rev. E* **2009**, *80*, 021931.
(10) Corvera, E.; Mouritsen, O. G.; Singer, M. A.; Zuckermann, M. J. The permeability and the effect of acyl-chain length for phospholipid bilayers containing cholesterol: Theory and experiments. *Biochim. Biophys. Acta* **1992**, *1107*, 261–270.
(11) Saito, H.; Shinoda, W. Cholesterol effect on water permeability through DPPC and PSM lipid bilayers: A molecular dynamics study. *J. Phys. Chem. B* **2011**, *115*, 15241–15250.
(12) Simons, K.; Ikonen, E. Functional rafts in cell membranes. *Nature* **1997**, *387*, 569–572.
(13) Lingwood, D.; Simons, K. Lipid rafts as a membrane-organizing principle. *Science* **2010**, *327*, 46–50.
(14) Sonnino, S.; Prinetti, A. Membrane domains and the "lipid raft" concept. *Curr. Med. Chem.* **2013**, *20*, 4–21.
(15) Pokorny, A.; Yandek, L. E.; Elegbede, A. I.; Hinderliter, A.; Almeida, P. F. F. Temperature and composition dependence of the interaction of δ-lysin with ternary mixtures of sphingomyelin/cholesterol/POPC. *Biophys. J.* **2006**, *91*, 2184–2197.
(16) Brender, J. R.; McHenry, A. J.; Ramamoorthy, A. Does cholesterol play a role in the bacterial selectivity of antimicrobial peptides? *Front. Inmunol.* **2012**, *3*, 1–4.
(17) Losada-Pérez, P.; Khorshid, M.; Hermans, C.; Robijns, T.; Peeters, M.; Jiménez-Monroy, K. L.; Truong, L. T. N.; Wagner, P. Melittin disruption of raft and non-raft-forming biomimetic membranes: A study by quartz crystal microbalance with dissipation monitoring. *Colloids Surf. B, Biointerfaces* **2014**, *123C*, 938–944.
(18) Tsukamoto, M.; Kuroda, K.; Ramamoorthy, A.; Yasuhara, K. Modulation of rafts domains in a lipid bilayer by boundary-active curcumin. *Chem. Commun.* **2014**, *50*, 3427–3430.
(19) Hamada, T.; Morita, M.; Kishimoto, Y.; Komatsu, Y.; Vestergaard, M.; Takagi, M. Biomimetic microdoplet membrane interface: Detection of the lateral localization of amyloid beta peptides. *J. Phys. Chem. Lett.* **2009**, *1*, 170–173.
(20) Kato, A.; Tsuji, A.; Yanagisawa, M.; Saeki, D.; Kazuhiko, J.; Yasunori, M.; Yoshikawa, K. Phase separation on a phospholipid membrane inducing a characteristic location of DNA accompanied by its structural transition. *J. Phys. Chem. Lett.* **2010**, *1*, 3391–3395.
(21) Privalov, P. L.; Plotnikov, V. V.; Filimonov, V. V. Precision scanner microcalorimeter for the study of liquids. *J. Chem. Thermodyn.* **1975**, *7*, 41–47.
(22) Mabrey, S.; Mateo, P. I.; Sturtevant, J. M. High-sensitivity scanning calorimetric study of mixtures of cholesterol with dimyristoyl- and dipalmitoylphosphatidylcholines. *Biochemistry* **1978**, *17*, 2464–2468.

DOI: 10.1021/acs.jpcb.5b00712
J. Phys. Chem. B 2015, 119, 4985–4992

(23) McMullen, T. P. W.; Lewis, R. N. A. H.; McElhany, R. N. Differential scanning calorimetric study of the effect of cholesterol on the thermotropic phase behavior of a homologous series of linear saturated phosphatidylcholines. *Biochemistry* **1993**, *32*, 516−522.
(24) Halstenberg, S.; Heimburg, T.; Hianik, T.; Kaatze, U.; Krivanek, R. Cholesterol-induced variations in the volume and enthalpy fluctuations of lipid bilayers. *Biophys. J.* **1998**, *75*, 264−271.
(25) Mannock, D. A.; Lewis, R. N. A. H.; Cullis; McElhany, R. N. A calorimetric and spectroscopic comparison of the effects of ergosterol and cholesterol on the thermotropic phase behavior and organization of dipamitoylphosphatidylcholine bilayer membranes. *Biochim. Biophys. Acta* **2010**, *1798*, 376−388.
(26) Jacobs, R.; Olfield, E. G. Deuterium nuclear magnetic resonance investigation of dimyristoil lecithin- and dipamitoyllecithin-cholesterol mixtures. *Biochemistry* **1979**, *18*, 3280−3285.
(27) Vist, M. R.; Davis, J. H. Phase equilibria cholesterol/dipalmitoylphosphatidylcholine mixtures: 2H nuclear magnetic resonance and differential scanning calorimetry. *Biochemistry* **1990**, *29*, 451−464.
(28) Sankaram, M. B.; Thompson, T. E. Cholesterol-induced fluid-phase immiscibility in membranes. *Proc. Natl. Acad. Sci. U.S.A.* **1991**, *88*, 8686−8690.
(29) Ramamoorthy, A.; Lee, D. K.; Narasimhaswamy, T.; Nanga, R. P. R. Cholesterol reduces pardaxin's dynamics−a barrel-stave mechanism of membrane disruption investigated by solid state NMR. *Biophys. Biochim. Acta* **2010**, *1798*, 223−227.
(30) McHenry, A. J.; Sciacca, M. F. M.; Brender, J. F.; Ramamoorthy, A. Does cholesterol supress the antimicrobial peptide induced disruption of lipid raft containing membranes? *Biophys. Biochim. Acta* **2012**, *1818*, 3019−3024.
(31) de Meyer, F.; Smit, B. Effect of cholesterol on the structure of a phospholipid bilayer. *Proc. Natl. Acad. Sci. U. S. A.* **2009**, *106*, 3654−3658.
(32) Nagle, J. F.; Nagle, S. T. Structure of lipid bilayers. *Biochim. Biophys. Acta* **2000**, *1469*, 159−195.
(33) Ivankin, A.; Kuzmenko, I.; Gidalevitz, D. Cholesterol-phospholipid interactions: new insights from surface X-ray scattering data. *Phys. Rev. Lett.* **2010**, *104*, 108101.
(34) Baumgart, T.; Hunt, G.; Farkas, E. R.; Webb, W. W.; Feigenson, G. W. Fluorescence probe partitioning between Lo/Ld phases in lipid membranes. *Biochim. Biophys. Acta* **2010**, *1768*, 2182−2194.
(35) El-Sayed, M. Y.; Guion, T. A.; Fayer, M. D. Effect of cholesterol on viscoelastic properties of dipalmitoylphosphatidylcholine multibilayers as measured by laser-induced ultrasonic probe. *Biochemistry* **1986**, *25*, 4285−4832.
(36) Mioshy, T.; Lönnfors, M.; Slotte, J. P.; Kato, S. A detailed analysis of partial molecular volumes in DPPC/cholesterol lipid bilayers. *Biochim. Biophys. Acta* **2014**, *1838*, 3069−3077.
(37) Bennet, W. F. D.; MacCallum, J. L.; Tieleman, D. P. Thermodynamic analysis of the effect of cholesterol on dipamitoylphosphatidylcholine lipid membranes. *J. Am. Chem. Soc.* **2009**, *131*, 1972−1978.
(38) Joannis, J.; Coppock, P. S.; Yin, F.; Mori, M.; Zamorano, A.; Kindt, J. T. Atomistic simulation of cholesterol effects on miscibility of saturated and unsaturated phospholipids: implications for liquid-ordered/liquid-disordered phase coexistence. *J. Am. Chem. Soc.* **2011**, *113*, 3625−3634.
(39) Almeida, P. F. A simple themodynamic model of the liquid-ordered state and the interactions between phospholipids and cholesterol. *Biophys. J.* **2011**, *100*, 420−429.
(40) Ipsen, J. H.; Karlström, G.; Mouritsen, O. G.; Wennerström, H.; Zuckermann, M. J. Phase equilibria in the phosphatidylcholine-cholesterol system. *Biochim. Biophys. Acta* **1987**, *905*, 162−172.
(41) Mouritsen, O. G. The liquid-ordered state comes of age. *Biochim. Biophys. Acta* **2010**, *1798*, 1286−1288.
(42) Hirst, L.; Uppamoochikkal, P.; Lor, C. Phase separation and critical phenomena in biomimetic ternary lipid mixtures. *Liq. Cryst.* **2011**, *38*, 1735−1747.
(43) Castellana, E. T.; Cremer, P. S. Solid supported lipid bilayers: From biophysical studies to sensor design. *Surf. Sci. Rep.* **2006**, *61*, 429−444.
(44) Redondo-Morata, L.; Giannotti, M. I.; Sanz, F. Influence of cholesterol on the phase transition of lipid bilayers: A temperature-controlled force spectroscopy study. *Langmuir* **2012**, *28*, 12851−12860.
(45) Wang, J.; Liu, K. W.; Segatori, L.; Biswal, S. L. Lipid bilayer transformations detected using microcantilevers. *J. Phys. Chem. B* **2014**, *118*, 171−178.
(46) Keller, C. A.; Kasemo, B. Surface specific kinetics of vesicle adsorption measured with a quartz-crystal microbalance. *Biophys. J.* **1998**, *75*, 1397−1402.
(47) Cho, N. J.; Frank, C. W.; Kasemo, B.; Höök, F. Quartz crystal microbalance with dissipation monitoring of supported lipid bilayers on various substrates. *Nat. Protoc.* **2010**, *5*, 1096−1106.
(48) Dixon, M. C. Quartz crystal microbalance with dissipation monitoring: enabling real-time characterization of biological materials and their interactions. *J. Biomol. Technol.* **2008**, *19*, 151−158.
(49) Ohlsson, G.; Tigerström, A.; Höök, F.; Kasemo, B. Phase transitions in adsorbed lipid vesicles measured using a quartz crystal microbalance with dissipation monitoring. *Soft Matter* **2011**, *7*, 10479−10755.
(50) Losada-Pérez, P.; Jiménez-Monroy, K. L.; van Grinsven, B.; Leys, J.; Janssens, S. D.; Peeters, M.; Glorieux, C.; Thoen, J.; Haenen, K.; De Ceuninck, W.; et al. Phase transitions in lipid vesicles detected by a complementary set of methods: heat-transfer measurements, adiabatic scanning calorimetry and dissipation-mode quartz crystal microbalance. *Phys. Stat. Sol. A* **2014**, *21*, 1377−1388.
(51) Jing, Y.; Kunze, A.; Svedhem, S. Phase transition-controlled flip-flop in asymmetric lipid membranes. *J. Phys. Chem. B* **2014**, *118*, 2389−2395.
(52) Jing, Y.; Trefna, H.; Persson, M.; Kasemo, B.; Svedhem, S. Formation of supported lipid bilayers on silica: relation to the lipid phase transition temperature and liposome size. *Soft Matter* **2014**, *10*, 187−195.
(53) Wargenau, A.; Tufenkji, N. Direct detection of the gel-fluid phase transition of a single supported phospholipid bilayer using quartz crystal microbalance with dissipation monitoring. *Anal. Chem.* **2014**, *86*, 8017−8020.
(54) Losada-Pérez, P.; Mertens, N.; de Medio-Vasconcelos, B.; Slenders, E.; Leys, J.; Peeters, M.; van Grinsven, B.; Gruber, J.; Glorieux, C.; Pfeiffer, H. Phase transitions of binary lipid mixtures: a combined study by adiabatic scanning calorimetry and quartz crystal microbalance with dissipation. *Adv. Condens. Matter Phys.* **2015**, 479318 DOI: 10.1155/2015/479318.
(55) Voinova, M. V.; Jonson, M.; Kasemo, B. Dynamics of viscous amphiphilic films supported by elastic solid substrates. *J. Phys.: Condens. Matter* **1997**, *9*, 7799−7808.
(56) Cho, N. J.; Kanazawa, K. K.; Glenn, J. S.; Frank, C. W. Employing two different quartz crystal microbalance models to study changes in viscoelastic behavior upon transformation of lipid vesicles to a bilayer on a gold surface. *Anal. Chem.* **2007**, *79*, 7027−7035.
(57) Reimhult, E.; Höök, F.; Kasemo, B. Intact vesicle adsorption and supported biomembrane formation from vesicles in solution: Influence of surface chemistry, vesicle size, temperature, and osmotic pressure. *Langmuir* **2003**, *19*, 1681−1691.
(58) Sundh, M.; Svedhem, S.; Sutherland, D. Influence of phase separating lipids on supported lipid bilayer formation at SiO_2 surfaces. *Phys. Chem. Chem. Phys.* **2010**, *12*, 453−460.
(59) Serro, A. P.; Carapeto, A.; Paiva, G.; Farinha, J. P. S.; Colaço, R.; Saramago, B. Formation of an intact liposome layer adsorbed on oxidized gold confirmed by three complementary techniques: QCM-D, AFM, and confocal fluorescence microscopy. *Surf. Int. Anal.* **2012**, *44*, 426−433.
(60) Zammit, U.; Marinelli, M.; Mercuri, F.; Paoloni, S. Analysis of the order character of the R_{II}-R_I and the R_I-R_V phase transitions in alkanes by photopyroelectric calorimetry. *J. Phys. Chem. B* **2010**, *114*, 8134−8139.

DOI: 10.1021/acs.jpcb.5b00712
J. Phys. Chem. B 2015, 119, 4985−4992

(61) Yang, J.; Appleyard, J. The main phase transition of mica-supported phosphatidylcholine membranes. *J. Phys. Chem. B* **2000**, *104*, 8097−8100.
(62) Recktenwald, D. J.; McConnell, H. M. Phase equilibria in binary mixtures of phosphatidylcholine and cholesterol. *Biochemistry* **1981**, *20*, 4505−4510.
(63) de Meyer, F. J. M.; Benjamini, A.; Rodgers, J. M.; Misteli, Y.; Smit, B. Molecular simulation of the DMPC-cholesterol phase diagram. *J. Phys. Chem. B* **2010**, *114*, 10451−10461.

DOI: 10.1021/acs.jpcb.5b00712
J. Phys. Chem. B 2015, 119, 4985−4992